Environmental Earth Sciences (2018) 77:204
https://doi.org/10.1007/s12665-018-7350-5

ORIGINAL ARTICLE

Neogene clay and its relation to landslides in the southwestern Loess Plateau, China

J. S. Shi[1,2] · L. Z. Wu[3] · Y. X. Qu[1] · B. Li[1] · S. R. Wu[1]

Received: 21 February 2017 / Accepted: 18 February 2018 / Published online: 3 March 2018

Abstract

Loess occurs widely in Northwestern China, covering Neogene clay and other sedimentary units that overlie the bedrock. The Neogene clays of the Baoji Region of Shaanxi Province, north China, including the eolian Hipparion and paleo-Sanmen Lake fluvial deposits, are typical clays of the southern Chinese Loess Plateau. These clays are also sensitive key strata controlling the development of large-scale landslides along the slope of the loess tableland surrounding the Guanzhong Basin. To investigate the Neogene clay types and landslides in the region, soil samples were tested and the macro- and micro-structures of the clay strata were analyzed. Comprehensive analysis methods, including the pipette method and fine X-ray diffraction, were applied to quantitatively analyze the sample composition and determine the clay mineral types. The Neogene clays are mainly composed of illite and montmorillonite mixed-layer minerals. On the Williams' discrimination diagram of swelling potential, both types of clay are medium to strongly expansive soil. Two case studies illustrate that rainfall reduces the shear strength of the Neogene clay and raises the groundwater level. Rainfall has gradually destroyed the structure of the Neogene clay, transforming it to sliding belt soil. The sliding belt lies mainly within the Neogene clay layers, significantly affecting the occurrence and characteristics of landslides in Baoji. The rise in groundwater level and weakening of the shear strength of the Neogene clay are important factors in the occurrence of landslides. The long-term strength is a key factor affecting the development of loess landslides along the loess tableland in Baoji.

Keywords Neogene · Clay · Clay mineral · Swelling soil · Loess Plateau · Landslide

Introduction

The Neogene strata of the Chinese Loess Plateau consist of Hipparion red clay and lacustrine deposits of the ancient Sanmen Lake (known as the Sanmen Formation), which consists of a sequence of grayish-yellow clays, grayish-green clays, red clays, compact sandy clay, and sandy gravel underlying thick loess (Ding and Liu 1989). The Hipparion red clay is a red talus deposit characterized by abundance of the *Hipparion* fauna. The clay has been extensively used in studies of paleoenvironment and paleoclimate evolution, because it was identified as having the same eolian source as the overlying loess paleosol. Deposition of lake–river facies during the Sanmen period occurred mainly in the Guanzhong Basin of Shaanxi Province and western Henan, extending over Henan and Shanxi Provinces; the deposit is typical of the sediment of paleo-lake basins. The Hipparion red clay and the sedimentary strata of paleo-lake basins underlying the Chinese Loess Plateau are regarded as a special type of soil that plays an important role in the generation of landsides and affects the stability of the loess slopes in this area (Wang et al. 2001, 2011, 2014a, b; Tu et al. 2009; Zhang and Liu 2010; Xu et al. 2012, 2015; Peng et al. 2015; Sun et al. 2016; Wu et al. 2017a).

Loess overlying the paleo-lake sediments and red clay is widely distributed in northwestern China. The physical and mechanical properties of loess have been studied extensively (Derbyshire and Mellors 1988; Derbyshire et al. 1994, 1995, 2000; Dijkstra et al. 1994; Derbyshire 2001; Xu et al. 2012; Zhang et al. 2013). Large-scale loess landslides involve the overlying Neogene beds, in which sliding belts are found.

✉ L. Z. Wu
cewulz@gmail.com

[1] Institute of Geomechanics, Chinese Academy of Geological Sciences, Beijing 100081, China

[2] China Geological Survey, M.L.R, Beijing 100037, China

[3] State Key Laboratory of Geohazard Prevention and Geoenvironment Protection, Chengdu University of Technology, Chengdu 610059, Sichuan, China

Neogene clay can play a significant role in the formation of large-scale loess landslides. Such landslide processes affect the mechanical characteristics of the red clay and other sediments that may be covered by the loess (Qu et al. 1999). Geo-engineers generally refer to the Neogene beds as mudstone or interbedded sandy shale; however, the mudstone in this layer is also called "red clay." There are obvious mechanical differences between rock and soil, particularly for the clay layers. The clay minerals (type and content) have a significant impact on the engineering properties, especially the hydro-physical properties. The swelling clay minerals (montmorillonite and its mixed-layer minerals) are a key factor influencing the geological engineering properties.

Loess has a high shear strength and stiffness under unsaturated conditions and is significantly weakened when wet (Zhou et al. 2014). With a low water content, loess generally has enough shear strength to resist slope destabilization; however, the sediment shows a rapid decrease in shear strength once wetted (Derbyshire et al. 1994; Lin and Wang 1988). Matric suction (the difference between pore-air pressure and pore-water pressure in unsaturated soils) is dissipated during wetting, thus reducing shear strength. The shear strength of unsaturated loess is controlled by matric suction, which renders a loess slope temporarily safe.

Baoji City, located on the southern Loess Plateau, China, is part of the loess area; the loess is identified based on the loess grain-size classification method using the Casagrande aerometric method (Casagrande 1947). A total of 32 loess paleosol layers of Quaternary age with a maximum total thickness of 158.4 m are found in this region. Neogene red clay and sandy gravel interbedded with different sedimentary facies occur under those layers (Ding and Liu 1989; Yue 1996; Ding et al. 1997). Baoji is an area typical of the northwest Loess Plateau, which includes a large area of loess, red clay, and deposits formed in lacustrine facies (Figs. 1, 2; Yue 1996).

In recent years, the landslide hazards in the loess area in the western Guanzhong area have been investigated in detail. Field surveys indicated that almost 200 large-scale landslides have occurred along the margin of the loess tableland on the northern Wei River (Li et al. 2012). Moreover, the sliding area occupies most of the western area of the north bank. The sliding plane of the large-scale landslides lies in the Neogene clay (Li et al. 2012). As a result of the increase in rainfall infiltration and irrigation into the loess, the occurrence of landslides has increased (Derbyshire et al. 2000; Zhang et al. 2009; Xu et al. 2013); therefore, the mechanical features of the Neogene clay should be the key factors determining the occurrence of large-scale landslides in the Baoji area.

To investigate the effect of the mechanical properties of Neogene clay on landslides, the objective of this study was to analyze the mineral content, swelling potential, and mechanical properties of the Neogene clay that crops out or is buried along the slopes of the loess tableland, and the clay minerals and their composition in the Baoji area. Based on quantitative tests of the clay minerals of the Hipparion red clay and the Sanmen Formation, their swelling properties in the strata are discussed. The effect of the clay on landslide occurrence is analyzed using case studies of landslides.

Materials and methods

Regional setting

The Baoji area is located on the southern margin of the Loess Plateau (Fig. 1). The present climate is mildly humid, and the annual temperature range is 7.6–12.9 °C with an annual mean of 12 °C (25.4 °C in July). The mean annual precipitation is 710.24 mm. Up to 60% of the precipitation occurs between July and September.

Intense, uneven vertical fault-zone movement occurred during the Tertiary and continued until the beginning of the early Pleistocene. The movement uplifted the Qinling Mountains and the Ordos Plateau, and the Wei River basin was filled by 6000-m-thick Neogene deposits (Zhang et al. 1995). With a further uplift commencing at the end of the Pliocene, lacustrine deposits varying from clays to fluvial gravel and sand sequences, and alternating layers of argillites, arenites, and conglomerates were laid down. Because of the erosion of the Pliocene lacustrine basin by stream systems and reactivation of folds and faults, a very unstable base developed for the extensive Quaternary loess accumulations: This is part of the underlying cause of loess failure in the study area (Shi et al. 2016).

The main lithologies of the strata in the study area are Neogene argillites and fluvial deposits consisting of clayey silts, gravels, and Quaternary loess. In these units, the Neogene argillites are of particular significance for the study of the loess slides (Wang et al. 2011).

Methods

To understand the interaction between the Neogene clays and the landslides in the Guanzhong region, detailed field surveys were carried out in combination with QuickBird satellite imagery. To investigate the structure of landslides in the region, drilling was performed at ten field sites. There were 36 drills with a maximum depth of 198 m. Nine samples of Neogene clay were obtained, all from the slip surface or near the landslide failure surface. The samples (with particle size corresponding to colloidal particles, smaller than 0.002 mm) are listed in Table 1. The samples were analyzed using the pipette and dispersion methods (with

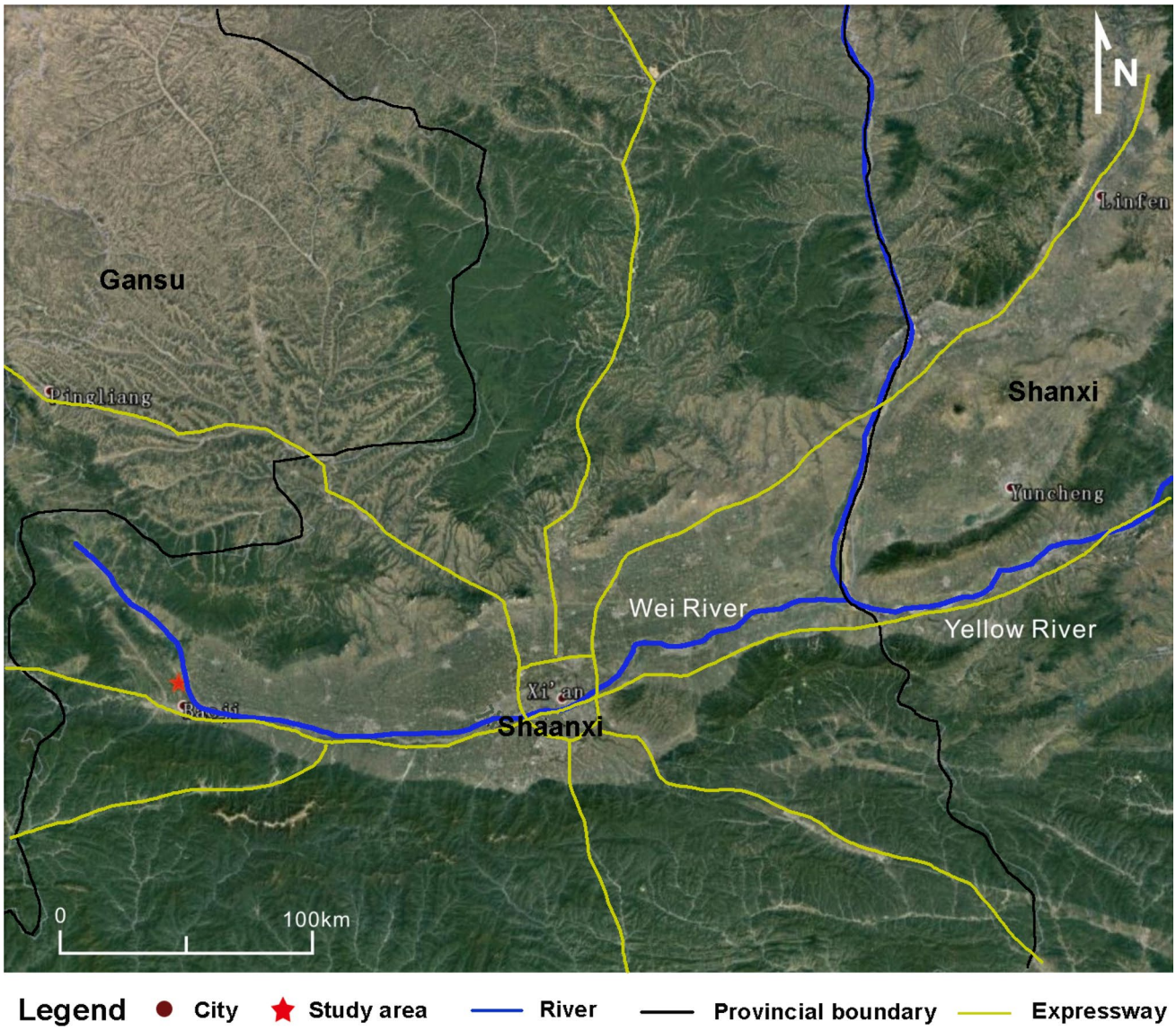

Fig. 1 Aerial photograph showing the study area, with important features marked

hydrogen peroxide to remove organic matter, accompanied by ultrasonication for 5 min; Buurman et al. 1997). The soil sampling locations are marked in Fig. 3. Specimens were collected from cores, which were 10 cm in diameter.

To determine the precise mineral composition of the Neogene hard clay, X-ray diffraction (XRD) was used to measure the abundances of the clay minerals montmorillonite and illite. The selective adsorption method with the organic dye methylene blue was also applied to analyze the effective montmorillonite content (Li et al. 2012). The swelling potential was calculated from the free swelling ratio, which is the ratio of the equilibrium soil volume of 10 g of oven-dried soil passed through a 425-μm sieve in distilled water to the equilibrium soil volume in carbon tetrachloride (Horpibulsuk et al. 2007). Certain properties of the Neogene hard clay from Baoji were measured following the Chinese Code for Investigation of Geotechnical Engineering (GB 50021-2001 2002) and the Chinese Technical Code for Buildings in Expansive Soil Regions (GB 50112-2013 2013). The Williams method together with plastic index, which is based on work from South Africa, has been adopted as the international method for determining swelling potential. Additionally, direct shear tests and ring tests with different values of water content were carried out to analyze the clay strength related to the landslides in the Guanzhong region. Two case studies were carried out using the Williams' discrimination diagram to illustrate the relationship between the Neogene clay and the landslides in the region.

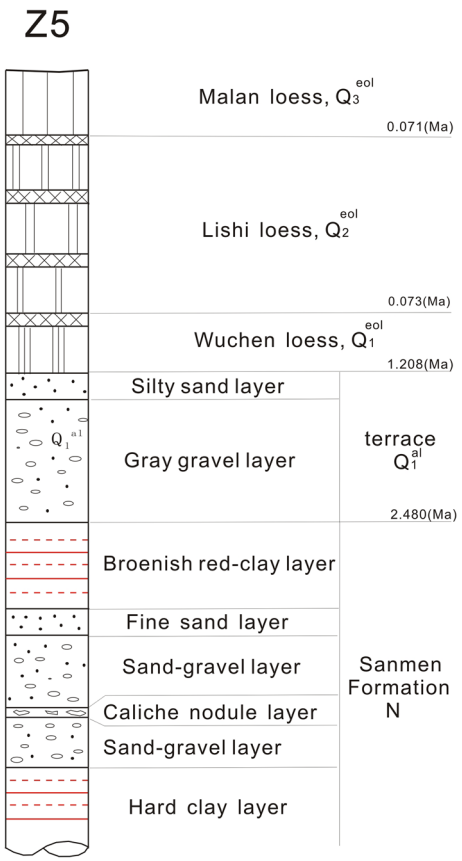

Fig. 2 Typical stratigraphic column through the loess and Neogene clay in Baoji

Distribution of sediment types

The main strata on the northern slope of Baoji consist of loess paleosol, Hipparion red clay, lacustrine facies deposits of the ancient Sanmen Lake, and underlying bedrock strata. This stratigraphic model is based on test results from borehole cores from the northern bank of the Wei River, Baoji, the distribution of the Wei River terraces, and the present regional topography shown in Fig. 3. The stratigraphic sequence of the study area is as follows: The Hipparion clay in the loess tableland and the overlying loess paleosol were deposited during a period of continuous sedimentation. The transitions between the different sedimentary facies of these strata are gradual; however, they show unconformable contacts in the hilly loess area. The ancient Sanmen Lake sedimentary units consist of the lower Pleistocene Sanmen and the Pliocene Youhe and Bahe Formations. The Sanmen Formation and Wucheng loess were deposited during the same period in different facies.

The Hipparion red clay in the Neogene strata is found mainly in the loess tableland on the northwest side, and generally shows a gradual transition to the overlying loess (sites No. 4 and 9 in Fig. 3). Residual erosion was observed in the hilly and mountainous loess area. The Sanmen Formation occurs mainly in the loess tableland. The loess tableland area is characterized by an increase in thickness from northwest to southeast, a decrease in the burial depth from northwest to southeast, and an alternating transitional phase in some sections with the Hipparion red clay covering the ancient Sanmen Lake sediments. The Sanmen Formation reveals the evolution of the extinction process of the ancient Sanmen Lake, which progressed from northwest to southeast, forming the Wei River valley, and finally the gradual formation of the ancient landforms.

The Hipparion red clay originated from dust sediment composed of homogeneous particles (Qu et al. 1999). In general, there is no sand or gravel in the deposit, only a gravel layer located at the bottom, which can be inferred to have partly undergone diagenesis because of the significant gray calcareous nodular layers formed by eluviation. Several dark brown iron/manganese films of eolian origin have formed at the surface and in joints or cracks in the soil where the bedding is not developed. In the stratigraphic sequence, the light red hard clay of the Sanmen Formation is generally interbedded with sand and gravel layers (Ding and Liu 1989). The surface of the clay strata is characterized by stratification and an erosional surface transformed

Table 1 Neogene clay composition and hydro-physical properties

Name of the clay	No.	Grain composition (mm%)			Montmorillonite (%)	Specific surface (m^2/g)	$CaCO_3$ (%)
		> 0.075	0.075–0.005	< 0.005			
Sanmen clay	1	2.07	55.80	42.13	22.33	236.42	1.67
	2	10.48	56.19	33.33	14.34	126.37	5.43
	6	12.80	54.92	32.28	13.91	148.30	1.48
	8	7.67	58.04	34.29	18.87	168.10	8.16
	10	1.51	54.17	44.32	15.91	154.50	–
Hipparion red clay	3	0.08	60.51	39.41	19.10	219.25	1.08
	5	3.41	55.90	40.69	23.74	258.27	6.32
	7	0.81	60.68	38.51	19.05	156.22	–
	9	7.40	60.17	32.43	18.49	206.98	9.00

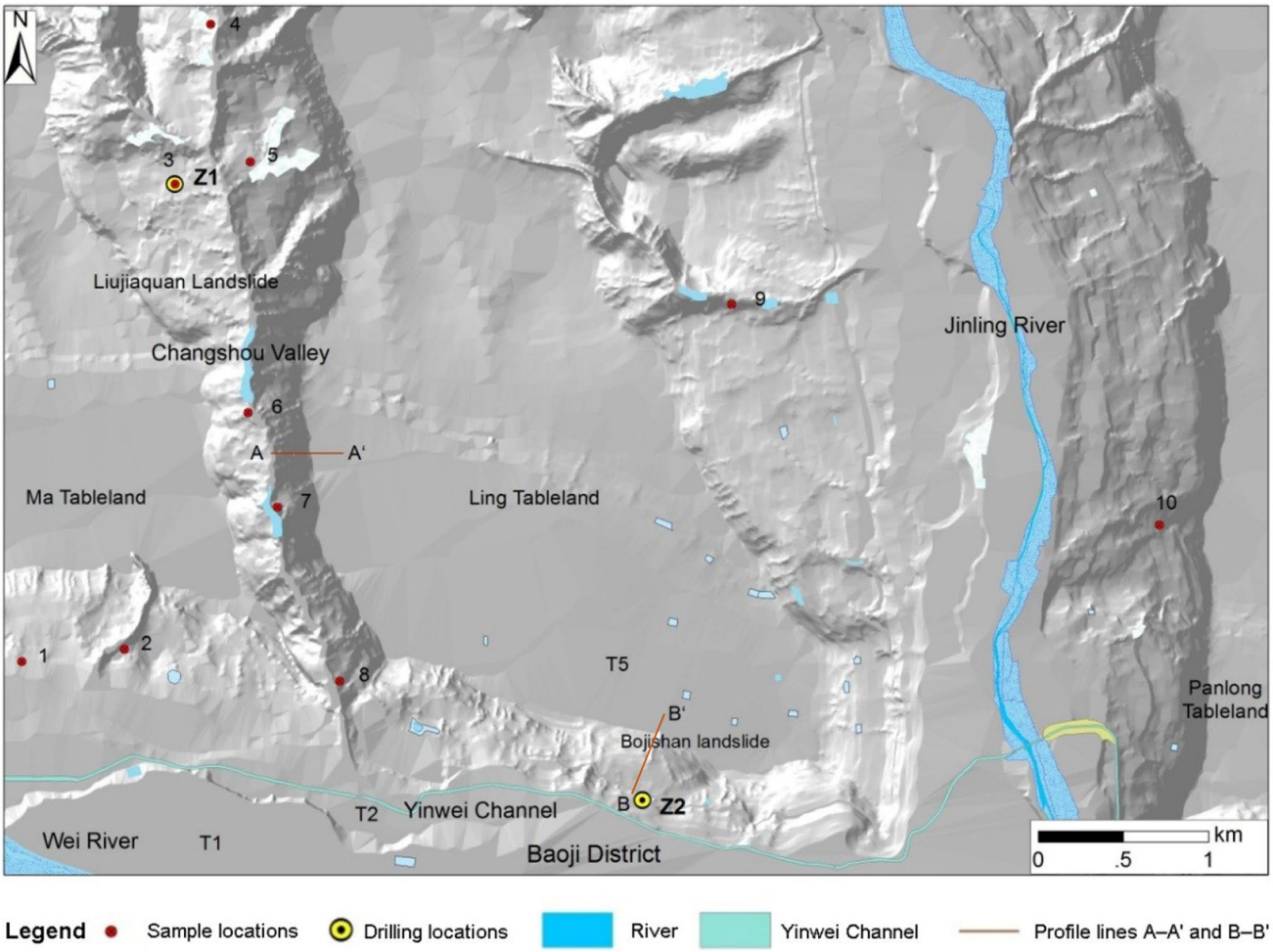

Fig. 3 Schematic illustration of Loess Plateau geomorphology in northern Baoji and locations of the Neogene clay sampling and drilling sites: 1: sample locations; 2: drilling locations; 3: river; 4: Yinwei Channel; 5: profile lines A–A′ and B–B′

by floods; the clay contains coarse sand (> 0.5 mm) and dust (> 2 mm), which is not present in the Hipparion red clay. Lacustrine sediments with clear bedding and joint fissures were identified. The macrostructure is the main characteristic distinguishing the Hipparion red clay from the Sanmen hard clay. The Hipparion red clay has no bedding but has layered characteristics similar to the alternating sedimentary sequences in the loess paleosol, which consists of stripes of red "loess" and "ancient soil."

The slope regions generally show an unconformable contact between the Hipparion red clay and the overlying loess. The Hipparion red clay experienced strong weathering and erosion, forming a paleo-weathering crust at the surface. The weathering crust was then covered by loess or underwent shear rupturing caused by tectonics or a gravity-formed interlayer shear zone (Shi et al. 2016). Ultimately, these processes led to the formation of the sliding surface in this area. The sliding surface lies mostly in the Neogene clay; the overlying layers are composed of sand and gravel, or other sediments (Fig. 4).

Fig. 4 Sanmen Formation hard clay layer and the overlying sand and gravel layers

Physical and mechanical properties of the clay

Composition of clay samples

Both the Hipparion and Sanmen layers have high clay contents, ranging from 32.27 to 44.32%. The colloidal particle content is between 21.89 and 39.04%, as listed in Table 1. There is no clear difference in the clay and colloidal particles between the Hipparion red clay and the Sanmen clay. The specific surface area of the Hipparion red clay is higher than that of the Sanmen clay.

Clay minerals have a significant impact on engineering properties, with certain basic properties and types of clay mineral (montmorillonite and mixed-layer clay minerals) being key factors. The Hipparion red clay is composed mainly of mixed-layer illite and montmorillonite. The secondary clay mineral is illite containing kaolinite and chlorite (Fig. 5b). The results, including the single-mineral montmorillonite and the crystal layer content of the mineral montmorillonite in the mixed layer, are listed in Table 1.

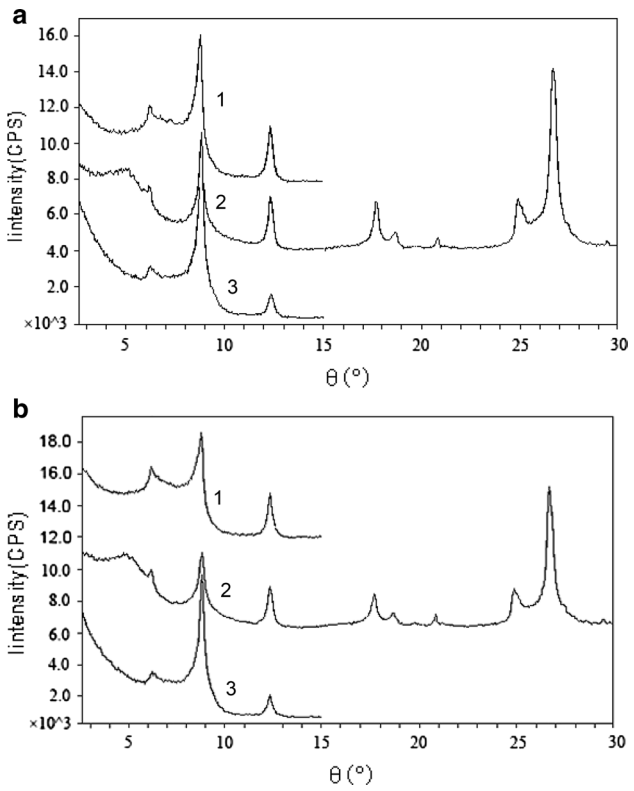

Fig. 5 XRD plots for Neogene clay, θ is the scanning angle of the device. **a** Sanmen clay (sample No. 9 in Fig. 3): (1) natural sample; (2) glycol-treated sample; (3) 550 °C heat-treated sample. **b** Hipparion red clay (sample No. 5 in Fig. 3): (1) natural sample; (2) glycol-treated sample; (3) 550 °C heat-treated sample

Overall, the content of the clay minerals and the XRD diffraction diagram indicate that the Hipparion red clay has a similar clay mineral content to the Sanmen clay, and there are no clear differences between samples obtained from different spatial positions and depths. The Hipparion red clay originated from dust sediment; the Sanmen clay from lacustrine sediment. Both types of clay were deposited after erosion and transportation (Li et al. 2012).

Swelling analysis of hard clay

The swelling potential can to some degree reflect the basic characteristics of the clay minerals, the composition in terms of particle sizes, and the clay ingredients of the exchanging cations. According to the Chinese Technical Code for Buildings in Expansive Soil Regions (GB 50112-2013 2013), clay with a free swelling ratio of $40 \leq \delta_{ef} < 65$ is low-swelling soil, medium-swelling soil has values of $65 \leq \delta_{ef} < 90$, and strongly expansive soil has $\delta_{ef} \geq 90$. The free swelling ratio of the Neogene hard clay ranged from 33 to 76%; thus, this clay is weak-to-medium-swelling soil. The swelling force is divided into four categories: low, medium (plastic index of 18.89–23.67), strong (plastic index of 25.88–31.62), and very strong (Fig. 6) (Williams and Donaldson 1980).

Shear strength

The results of direct shear tests indicate no correlation between the residual strength of the cohesive soil and the

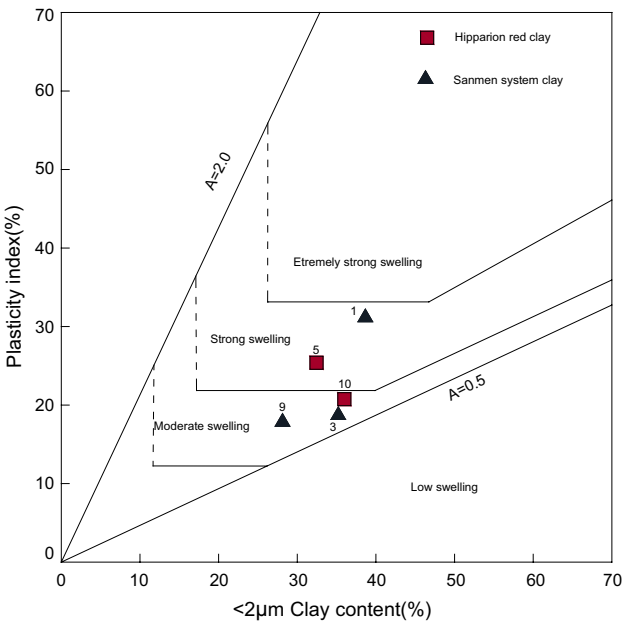

Fig. 6 Williams' swelling power discrimination diagram for Neogene hard clay. Reproduced with permission from Williams and Donaldson (1980)

water content. The residual strength decreases with increasing clay content of the soil. The unconfined compressive strength is commonly used in engineering for hardness classification of cohesive soils. In general, based on the direct shear results, the unconfined compressive strength of the saturated clays ranged from 0.3 to 1.5 MPa; the unsaturated shear strength was determined based on the cohesion and frictional angle from the direct shear results, together with the angle of shearing resistance with respect to the matric suction (Li et al. 2012). From the direct shear tests, the unconfined compressive strength of the Baoji Neogene hard clay and Hipparion red clay was 0.588–1.80 and 0.328–1.10 MPa, respectively. The clays are extremely hard soil but softer than extremely soft rock, and are thus classified as a transitional soil type known as hard clay.

Figure 7 describes the variations of shearing stress of the sliding belt with displacement under normal stresses of 400, 600, and 800 kPa. The residual strength of the sliding surface based on ring tests using a ring shear apparatus (Wile ARS-3, Germany) was approximately 80% of the peak strength (Fig. 7).

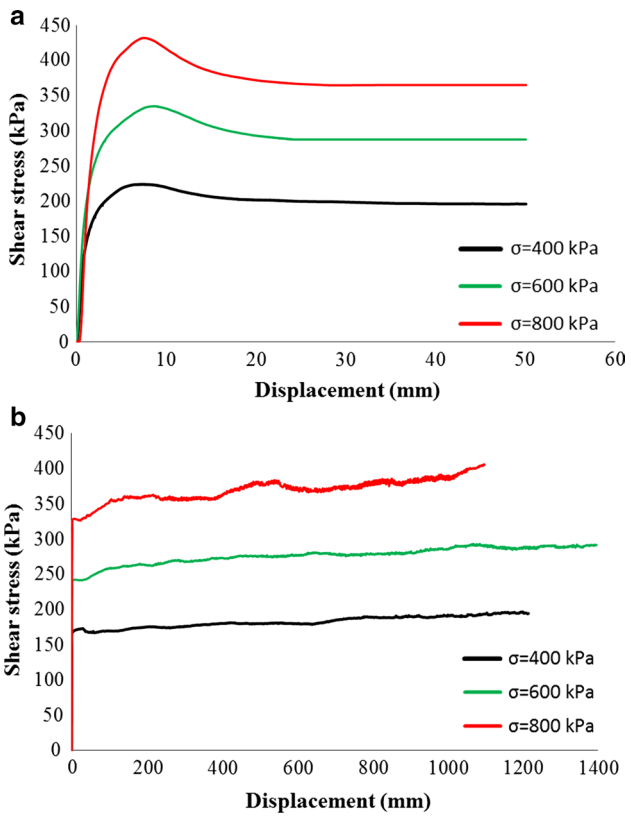

Fig. 7 Shear stress versus displacement for samples of Neogene clay from Baoji under different stress levels: **a** peak strength; **b** residual strength

Case studies

Changshou Valley landslide

The Neogene hard clay is located at the edge of the loess tableland in northern Baoji, where large-scale slides have occurred, mainly in the clay. The Neogene clay has been subjected to the long-term gravity forces of the high and steep slopes and to tectonic forces; this produced stress that was concentrated at the bottom of the slope, forming the interlayer zone. This zone provides a traceable surface for the sliding surface. The interlayer zone, along with an increase in tectonic activity and partial erosion of the Wei River during glacial and postglacial periods, caused the formation of the paleo-landslide. Large-scale slope failures at Baoji along the northern bank of the Wei River usually occur along the Sanmen clay. The sliding surfaces of some well-known landslides, such as the Bojishan landslide, are within or at the Sanmen clay layer. The Hipparion red clay is a potential sliding stratum located on both sides of the Jinling River and Changshou Valley (Fig. 3) because the Neogene hard clay usually crops out at the bases of the slopes. The Neogene hard clay is considered to be a typical confining bed and the main erosion strata of the rivers and valleys (Li et al. 2012). This clay has a higher natural shear strength than the upper loess paleosol but shows a remarkable decrease in shear strength when wetted or saturated. The unsaturated shear strength for the clay can be described as follows (Fredlund and Rahardjo 1993):

$$\tau = c' + (\sigma - u_a)\tan\phi' + (u_a + u_w)\tan\phi^b, \quad (1)$$

where σ is the total stress; u_a is the pore-air pressure; u_w is the pore-water pressure; $(u_a - u_w)$ is the matric suction; c' and ϕ' are the cohesion and frictional angles for saturated soils, respectively; and ϕ^b is the angle of shearing resistance with respect to matric suction, which increases with increasing matric suction (Fredlund and Rahardjo 1993). This angle increases nonlinearly with soil suction.

The soil slope stability in the regions was analyzed using the commercial software SLOPE/W (Geo-slope Ltd. 2007). The parameters of the profile are listed in Table 2 and were obtained from direct shear tests under drained conditions (Li et al. 2012). The initial water table is shown in Fig. 8. The pore-water pressure is zero at the left side of the model,

Table 2 Unsaturated shear strength parameters for Pliocene clay from the Changshou Valley

Clay type	Cohesion c' (kPa)	Frictional angle ϕ' (°)	Angle of shearing resistance with respect to matric suction ϕ^b (°)
Sanmen clay	32.6	17.4	15
Hipparion red clay	29.4	15.6	15

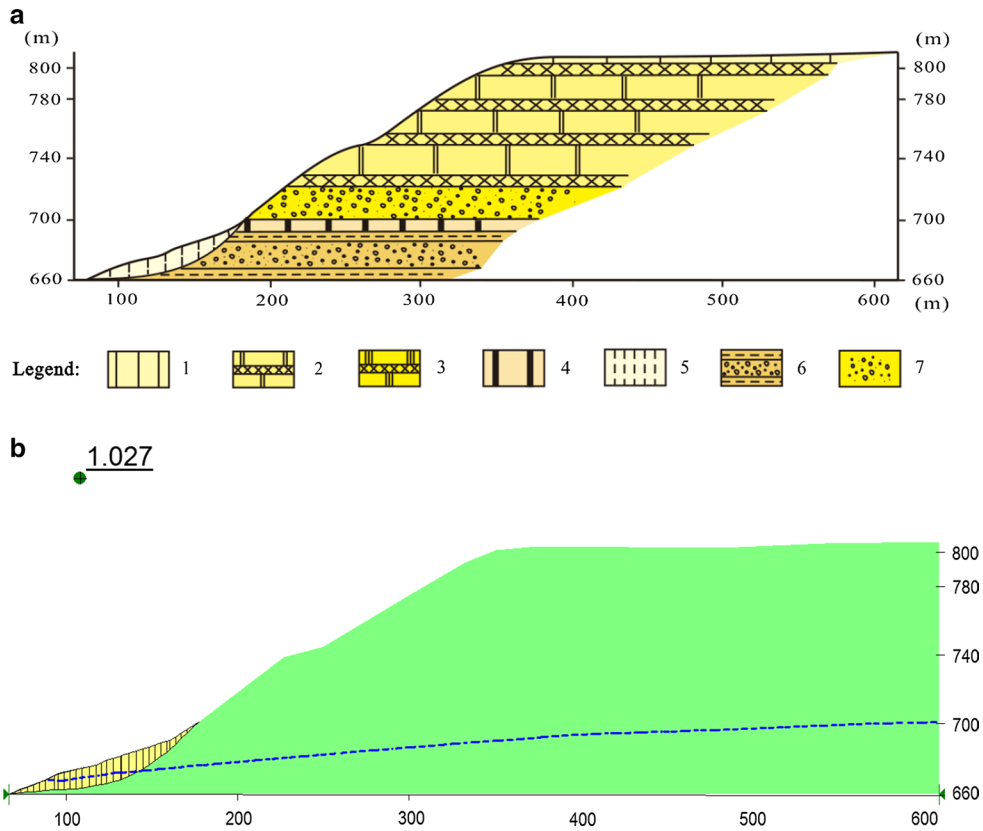

Fig. 8 Profile of the Changshou Valley along the line A–A′ marked in Fig. 2. **a** The profile: 1: Upper Pleistocene loess; 2: Middle Pleistocene loess; 3: Lower Pleistocene loess; 4: Hipparion red clay; 5: Landslide deposit; 6: Sanmen Formation clay; 7: River terrace. **b** The factor of safety and the potential sliding surface along profile A–A′ (Fig. 2)

and the pore-water pressure head is 40 m at the right side of the slope. The factor of safety (F_s) is 1.027, close to the threshold value. This factor was calculated using the residual strength parameters (Li et al. 2012) and $\phi^b = 15°$. The sliding surface is mainly located in the Sanmen Formation clay; some sliding occurs at the interface between the Sanmen clay and the Hipparion red clay. In Fig. 8, F_s of the slope under the initial groundwater table was obtained using SLOPE/W (Geo-slope Ltd. 2007). The initial F_s value is 1.03. When the groundwater table rises as a result of rainfall infiltration, F_s decreases to 0.99. Dissipation of matric suction or a rapid increase in the pore-water pressure in the slope causes a rapid decrease in the shear strength (Fredlund and Rahardjo 1993; Rahardjo et al. 1995). Thus, rainfall causes deterioration of the shear strength of the water-sensitive Neogene clay.

Bojishan landslide

The Bojishan landslide is situated in the northern part of central Baoji. The landslide is located in the loess tableland slope belt, which has an elevation of 550–880 m above sea level and a maximum distance from base to top of 320 m. The landslide material is made up of, from top to bottom, loose Quaternary loess, a layer of the Wei River (T5) gravel, and a layer of Sanmen clay and sandy gravel (Fig. 9). The Quaternary loess and paleosol on the top is 80 m thick. The gravel layer of the Wei River (T5) is approximately 15 m thick with an approximate volume of 2100×10^4 m^3 and is well cemented. The clay and sand gravel of the Sanmen Formation at the bottom of the slope is 44.2 m thick. The sandy gravel layer is the main aquifer in the tableland; the core sample from site No. 5 showed an underground water level of 60–75 m (Fig. 9b). Cracks appeared in the front of the Bojishan landslide in August 1981, and have been deforming continuously since then. More than 13 cracks have appeared in the landslide with a maximum crack width of 0.4 m; this poses a serious threat to the safety of residents in northern Baoji, Shaanxi Province. The direction of the Bojishan landslide was north–south, with the scarp located in the front of layer T5, in the floodplain. The landslide has an overall rectangular form. The east–west length of the slide is 280 m, and the north–south length is 350 m (Fig. 9). The main direction of the new and old landslides is 198° with a gradient of 20°–30°. A complete multistage arc-sliding boundary appeared. The sliding surface in the middle of the landslide was approximately horizontal, and developed within the hard sandy gravel layer. The dip angle of the shear outlet at the leading edge was about 25°, and a steep, circular sliding surface developed in the scarp of the landslide. The sliding bed is the Sanmen sandy gravel layer, which was influenced by the nearly horizontal strata.

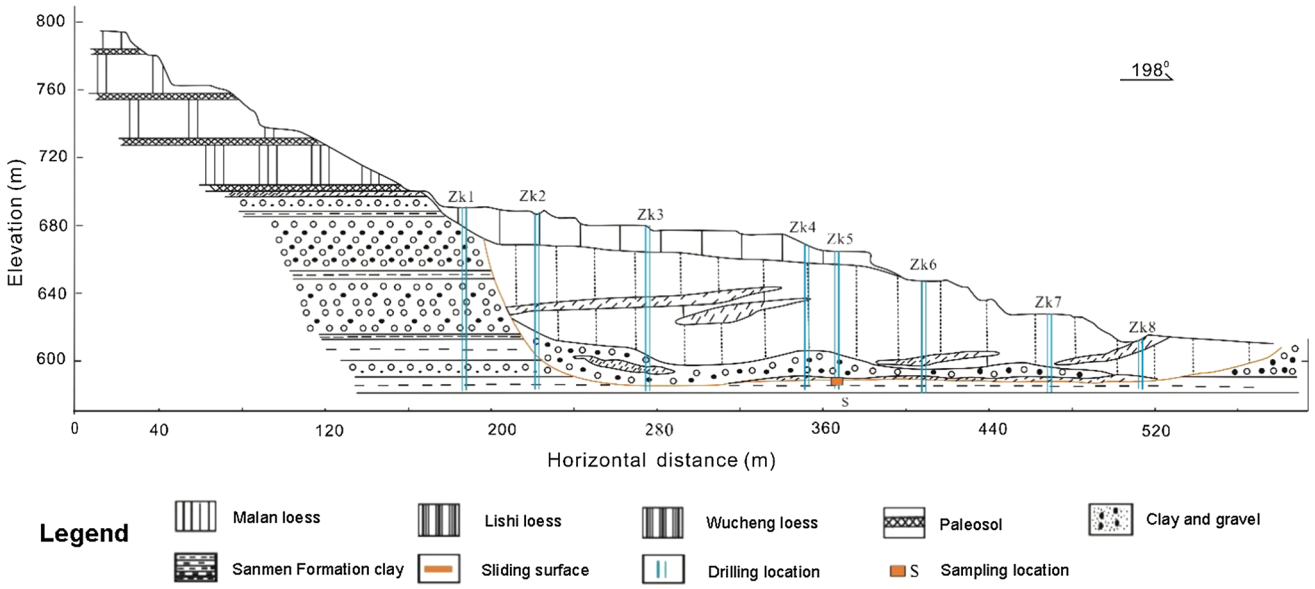

Fig. 9 Bojishan landslide. Stratigraphic section along profile B–B′ (marked in Fig. 2) of the Bojishan landslide

The groundwater of the Bojishan landslide has been continuously monitored since 2012 (Fig. 10). Figure 10 displays variations in the pore-water pressure of the Bojishan landslide during 2012. During the rainy season (May–October), the pore-water pressure increased; from October to December the pore-water pressure decreased. Most of the groundwater affecting the landslide is derived from rainfall. The stability of the landslide is controlled mainly by continuous heavy rain (Wu et al. 2017a, b).

The progress of the Bojishan landslide was closely linked to crack evolution. Cracks appeared in the sliding belt and the number of cracks gradually increased, which caused slow deformation. Subsequently, the sliding belt enhanced the seepage of groundwater and accelerated the interaction of the groundwater with external substances (Wang et al. 2011), which caused clay minerals such as montmorillonite to swell and the activity of the sliding belt to increase (Li et al. 2012). The formation of the sliding belt in the Sanmen clay involved complex physical and chemical processes (Li et al. 2012).

The creep deformation characteristics of the sliding belt were closely related to the stability of the landslide (van Asch et al. 2007). The development of micro-cracks in the slope corresponded to the creep deformation of the landslide (Bruckl and Parotidis 2005). During this process, the long-term strength was a key factor. After entering the stage of

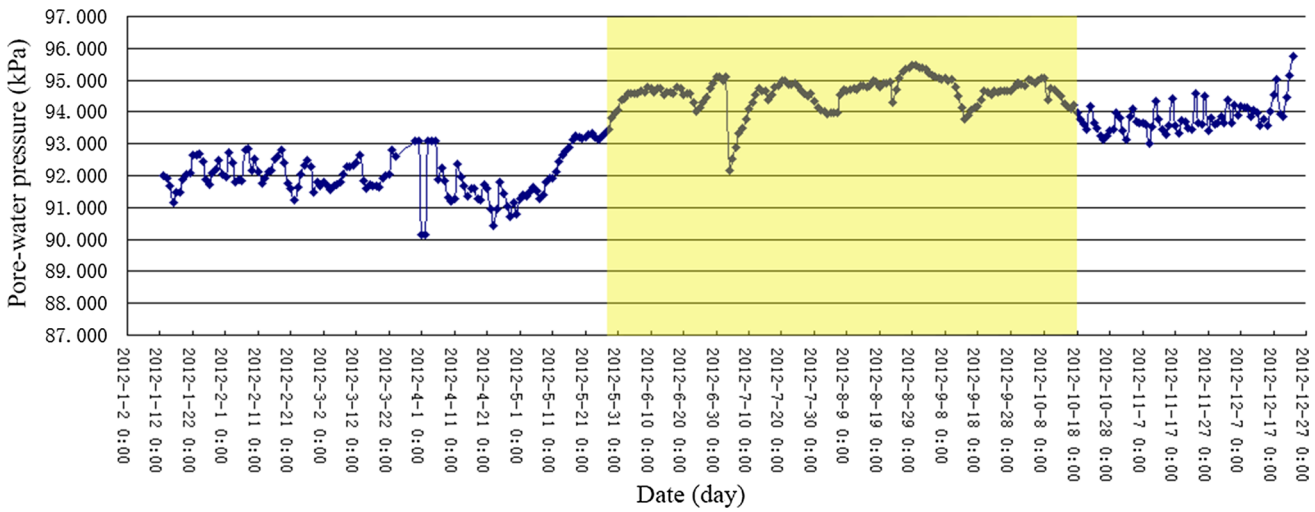

Fig. 10 Pore-water pressure–time curve for drilling site ZK5 of the Bojishan landslide

creep deformation, the stability of the landslide depended on the long-term strength of the sliding belt. The large deformation of the landslide mass was caused by the long-term creep accompanied by an increase in the water content of the sliding belt. During this creep, the structure of the clay was destroyed, and it was transformed into sliding belt soil; in this way, the plastification and stratification of the sliding belt were enhanced. The structures of the sliding belt were affected by the material composition, stress state, and groundwater environment. Variation in the moisture content of the Sanmen clay was related to crack occurrence; a rise in groundwater intensifies creep acceleration of the Sanmen clay.

Subsequently, changes in the groundwater level were important factors causing deformation of the Bojishan landslide. Weakening in the strength of the sliding belt was also a key factor controlling the slope stability. Furthermore, groundwater was identified as a significant contributor to the occurrence of many landslides in Baoji (Shi et al. 2016).

In the two case studies, water plays a significant role in the slope stability in the region. Rainfall infiltration reduced the shear strength of the partially saturated Neogene clay, causing a rise in the groundwater level in slopes consisting of water-sensitive Neogene clay. The sliding belt is mainly located within the Neogene clay layers (Fig. 8a): This clay plays a key role in controlling the slope stability in Baoji. Thus, slopes with particular structures associated with Neogene clay in Baoji are prone to sliding during rainfall events.

Conclusions

The underlying Neogene hard clay of the loess tableland in Baoji consists of Hipparion red clay and lacustrine facies Sanmen clay, which originated from the same substance. The clays are mainly composed of mixed-layer illite and montmorillonite, which exhibit little difference in particle size, clay content, and composition. The deposit was categorized as swelling clay because of the high effective content of montmorillonite. Our analysis indicates that the soil samples are mainly of medium-swelling type.

In the Baoji area, the potential sliding strata of the large-scale slopes are located in the Neogene clay. Neogene clay has a significant effect on the occurrence and characteristics of landslides in Baoji. The Neogene hard clay in Baoji is sensitive to water; therefore, a rainfall event can cause the clay to readily swell and disintegrate. This causes destruction of the soil structure and a severe decrease in soil strength, resulting in deformation, leading to slope failure in the loess area (Xu et al. 2013). The formation of the sliding belt in the Sanmen clay involved complex physical processes. Changes in the groundwater level and weakening of the strength of the sliding belt were important factors causing deformation of landslides in Baoji.

Acknowledgements We thank the National Natural Science Foundation of China (Grant Nos. 41372374 and 40802085), the National Science and Technology Support Program of China (Grant No. 2012BAK10B02), and the Creative Research Groups of China (Grant No. 41521002). We are also grateful to the Innovative Team of the Chengdu University of Technology.

References

Bruckl E, Parotidis M (2005) Prediction of slope instabilities due to deep-seated gravitational creep. Nat Hazards Earth Syst Sci 5(2):155–172

Buurman P, Pape T, Muggler CC (1997) Laser grain-size determination in soil genetic studies 1: practical problems. Soil Sci 162:211–218

Casagrande A (1947) Classification and identification of soils. Proc Am Soc Civ Eng 78:783–810

Derbyshire E (2001) Geological hazards in loess terrain, with particular reference to the loess regions of China. Earth Sci Rev 54:231–260

Derbyshire E, Mellors TW (1988) Geological and geotechnical characteristics of some loess and loessic soils from China and Britain: a comparison. Eng Geol 25:135–175

Derbyshire E, Dijkstra TA, Smalley IJ, Li Y (1994) Failure mechanisms in loess and the effects of moisture content changes on remoulded strength. Quat Int 24:5–15

Derbyshire E, Van Asch T, Billard A, Meng X (1995) Modelling the erosional susceptibility of landslide catchments in thick loess: Chinese variations on a theme by Jan de Ploey. CATENA 25:315–331

Derbyshire E, Meng XM, Dijkstra TA (2000) Landslides in the thick loess terrain of north-west China. Wiley, Chichester, pp 1–256

Dijkstra TA, Rogers CDF, Smalley IJ (1994) The loess of north-central China: geotechnical properties and their relation to slope stability. Eng Geol 36:153–171

Ding ZL, Liu DS (1989) Progresses of loess research in China (part I): loess tratigraphy. Quat Sci 9(1):24–35

Ding ZL, Sun JM, Zhu RX, Guo B (1997) Eolian origin of the red clay deposits in the loess plateau and implications for pliocene climatic changes. Quat Sci 2:147–156

Fredlund DG, Rahardjo H (1993) Soil mechanics for unsaturated soils. Wiley, New York

GB 50021-2001 (2002) Chinese code for geotechnical engineering investigation. China Architecture and Building Press, Beijing

GB 50112-2013 (2013) Technical code for buildings in expansive soil regions. China Planning Press, Beijing

Geo-slope Ltd (2007) Slope/W for slope stability analysis: user's guide. Geo-slope Ltd, Calgary

Horpibulsuk S, Shibuya S, Fuenkajorn K, Katkan W (2007) Assessment of engineering properties of Bangkok clay. Can Geotech J 44(2):173–187

Li B, Wu SR, Shi JS (2012) Research and analysis on large-scale loess landslides in loess tableland area of Weibei. Res Soil Water Conserv 19(1):206–211 **(in Chinese)**

Lin ZG, Wang SJ (1988) Collapsibility and deformation characteristics of deep-seated loess in China. Eng Geol 25:271–282

Peng JB, Fan ZJ, Wu D, Zhuang JQ, Dai FC, Chen WW, Zhao C (2015) Heavy rainfall triggered loess–mudstone landslide and subsequent debris flow in Tianshui, China. Eng Geol 186(24):79–90

Qu YX, Zhang YS, Qin ZM (1999) Hipparion laterite and landslide hazards on loess plateau of northwestern China. J Eng Geol 7(3):257–265 **(in Chinese)**

Rahardjo H, Lim TT, Chang MF, Fredlund DG (1995) Shearstrength characteristics of a residual soil. Can Geotech J 32(1):60–77

Shi JS, Wu LZ, Wu SR, Li B, Wang T, Xin P (2016) Analysis of the causes of large-scale loess landslides in Baoji, China. Geomorphology 264:109–117

Sun P, Peng JB, Chen LW, Lu QZ, Igwe O (2016) An experimental study of the mechanical characteristics of fractured loess in western China. Bull Eng Geol Environ 75(4):1639–1647

Tu XB, Kwong AKL, Dai FC, Tham LG, Min H (2009) Field monitoring of rainfall infiltration in a loess slope and analysis of failure mechanism of rainfall-induced landslides. Eng Geol 105:134–150

van Asch ThWJ, Van Beek LPH, Bogaard TA (2007) Problems in predicting the mobility of slow-moving landslides. Eng Geol 91(1):46–55

Wang SM, Wu XH, Zhang ZK, Jiang FC, Xue B, Tong GB, Tian GQ (2001) Environmental changes of Sanmen lacustrine deposits and the Yellow River flows eastwards. Sci China Ser D 31:760–768

Wang HB, Zhou B, Wu SR, Shi JS (2011) Characteristic analysis of large-scale loess landslides: a case study in Baoji City of Loess Plateau of northwest China. Nat Hazards Earth Syst Sci 11:1829–1837

Wang JJ, Liang JY, Zhang HP, Wu Y, Lin X (2014a) A loess landslide induced by excavation and rainfall. Landslides 11(1):141–152

Wang GH, Zhang DX, Furuya G, Yang J (2014b) Pore-pressure generation and fluidization in a loess landslide triggered by the 1920 Haiyuan earthquake, China: a case study. Eng Geol 174(23):36–45

Williams AAB, Donaldson G (1980) Building on expansive soils in South Africa. In: Proceedings of the 4th international conference on expansive soils, Denver, vol 2, pp 834–838

Wu LZ, Zhou Y, Sun P, Shi JS, Liu GG, Bai LY (2017a) Laboratory characterization of rainfall-induced loess slope failure. CATENA 150:1–8

Wu LZ, Zhang LM, Zhou Y, Li BE (2017b) Analysis of multi-phase coupled seepage and stability in anisotropic slopes under rainfall condition. Environ Earth Sci 76(14):469

Xu L, Dai FC, Gong QM, Tham LG, Min H (2012) Irrigation-induced loess flow failure in Heifangtai Platform, north-west China. Environ Earth Sci 66:1707–1713

Xu L, Dai FC, Tu XB, Javed I, Woodard MJ, Jin YL, Tham LG (2013) Occurrence of landsliding on slopes where flowsliding had previously occurred: an investigation in a loess platform, north-west China. CATENA 104:195–209

Xu XZ, Liu ZY, Xiao PQ, Guo WZ, Zhang HW, Zhao C, Yan Q (2015) Gravity erosion on the steep loess slope: behavior, trigger and sensitivity. CATENA 135:231–239

Yue LP (1996) Depositional relation between the loess, red clay and sedimtation of the lake-basin in the loess plateau. Acta Sedimentol Sin 14(4):148–153

Zhang MS, Liu J (2010) Controlling factors of loess landslides in western China. Environ Earth Sci 59:1671–1680

Zhang AL, Yang ZT, Zhong J, Mi FS (1995) Characteristics of late Quaternary activity along the southern border fault zone of Weihe graben basin. Quat Int 25:25–31

Zhang DX, Wang GH, Lou C, Chen J, Zhou Y (2009) A rapid loess flow slide triggered by irrigation in China. Landslides 6:55–60

Zhang F, Wang G, Kamai T, Chen W, Zhang D, Yang J (2013) Undrained shear behavior of saturated loess at different concentrations of sodium chlorate solution. Eng Geol 155:69–79

Zhou YF, Tham LG, Yan WM, Dai FC, Xu L (2014) Laboratory study on soil behavior in loess slope subjected to infiltration. Eng Geol 183:31–38